

Zero-point energy of a trapped ultracold Fermi gas at unitarity: squeezing the Heisenberg uncertainty principle and suppressing the Pauli principle to produce a superfluid state

D. K. Watson

Homer L. Dodge Department of Physics and Astronomy, University of Oklahoma, Norman, 73019, Oklahoma, USA.

Contributing authors: dwatson@ou.edu;

Abstract

The zero-point energy of a trapped ultracold Fermi gas at unitarity is investigated in relation to the combined effects of the Heisenberg uncertainty principle and the Pauli principle. This lowest allowed quantum state is a superfluid state which has been studied extensively both experimentally and theoretically. The method used for the current investigation is based on a recent series of papers that proposed microscopic dynamics based on normal modes to describe superfluidity instead of real-space Cooper pairs. This approach yielded excellent agreement with experimental data for multiple properties and allowed the microscopic behavior underlying these results as well as the basis of universal behavior to be analyzed in detail using the group theoretic basis of this general N-body approach. This microscopic picture is now used to elucidate the roles played by the uncertainty principle and the Pauli principle in determining the energy and character of the lowest allowed quantum state including the squeezed character of this superfluid state and the suppression of the Pauli principle.

Keywords: zero-point energy, Heisenberg uncertainty principle, Pauli principle, normal modes, collective phenomena, superfluidity

1 Introduction

Zero-point energy is defined as the lowest possible energy that a quantum system of particles may have consistent with the Heisenberg uncertainty principle. Even at absolute zero, quantum particles retain some motion, continuously fluctuating about values of the particles' positions and momentums as a consequence of their wave-like nature. This residual energy is known to result in measureable physical effects. For example, due to its large zero-point energy and low mass, helium remains a liquid down to absolute zero at standard atmospheric pressure. Other physical effects include spontaneous emission, the Lamb shift, the Casimir effect, and the magnetic moment of the electron. Zero-point energy is an important concept in multiple fields of physics affecting the discrepancy between the observed and calculated vacuum energy in cosmology[1], the validity of supersymmetry in high energy physics[2, 3], the fluctuating fields of quantum field theory[4] and offering a possible source of dark energy[1, 5]. Systems whose zero-point energy signatures have recently been studied include complex molecules[6], nanocrystals[7], optomechanical systems[8, 9], superconducting materials[10], and redshifted light from distant galaxies[11].

The ground state of ultracold Fermi gases has been studied extensively both experimentally and theoretically across the BCS to unitarity transition, i.e. from weak interactions limiting to the independent particle case to the strongly interacting unitary regime[12, 13, 14, 15, 16, 17, 18, 19, 20]. Theoretical descriptions of this transition can offer a test of the microscopic dynamics that underlie the evolution of the zero-point energy, i.e. the ground state energy of the system across this transition. As will be demonstrated in this study, both the uncertainty principle and the Pauli principle contribute to the changes in dynamics that are responsible for the character and energy of this lowest state and the emergence of superfluid behavior.

1.1 Background

Typically the ground state energy at zero temperature has been viewed theoretically as simply the lowest energy state of the relevant Hamiltonian chosen to describe this ultracold Fermi gas. In this work, I will view the ground state energy from a different perspective, that of the zero-point energy of a many-body system i.e. the minimum energy required to satisfy both the Heisenberg uncertainty principle and the Pauli principle for this system of identical fermions at zero temperature.

1) The Heisenberg uncertainty principle. - The zero-point energy is fundamentally a consequence of the Heisenberg uncertainty principle. Specifically, the uncertainty principle forbids complementary variables such as position and momentum (or energy and time) to be precisely specified by any quantum state. Therefore, the lowest energy state must have a distribution in position and momentum that satisfies the uncertainty principle, and thus its energy can never be zero even at a temperature of absolute zero. The product of the uncertainties for each particle in each dimension must obey:

$$\Delta x \Delta p \geq \hbar/2 \tag{1}$$

For a three-dimensional quantum harmonic oscillator, the product of the uncertainties in each dimension in the lowest state saturates this lower limit of the uncertainty

principle with the two uncertainties equal, i.e. with the same amount of uncertainty residing in the position of the particle and its momentum. This yields a zero-point energy of $3\hbar\omega_{ho}/2$ for each particle in this lowest state. This type of minimum uncertainty state with symmetric uncertainties is sometimes referred to as a coherent state. Higher states of the simple harmonic oscillator have larger values of both Δx and Δp as the energy of the state increases and the spatial extent of the wave function expands. For a many-body system of particles, each particle must individually satisfy the Heisenberg uncertainty principle.

Quantum states in which the uncertainty in one complementary variable has been reduced below the symmetric limit while the uncertainty in the other variable has increased such that the Heisenberg uncertainty principle is satisfied are called squeezed states. Such states have been known since the earliest days of quantum mechanics, have been used for decades in precision measurements in spectroscopy and interferometry including tests of fundamental physics, improvements in atomic clocks[21, 22, 23, 24, 25, 26, 27, 28] and improving the detection capabilities of gravitational-wave detectors[29, 30].

2) The Pauli principle. -The occupation of these states for independent, identical fermions in a harmonic well is, of course, determined by the Pauli principle; thus the lowest energy, i.e. the zero-point energy of an N-body system of identical fermions is controlled by the Pauli principle. The Pauli principle forbids two or more identical fermions, i.e. with all quantum numbers the same, from occupying the same quantum state. If two otherwise identical fermions have opposite spins, they may reside in the same quantum state, filling the allowed states two-by-two. This result can be compared to the situation for a system of identical non-interacting bosons in a three-dimensional harmonic trap all of which can occupy the lowest quantum state, so all the bosons in a N-body system can be in the minimum uncertainty state yielding a zero-point energy of $3N/2\hbar\omega_{ho}$. Thus we expect the zero-point energy of a system of identical non-interacting bosons to be much lower than the zero-point energy of a N-body system of identical non-interacting fermions each of which must obey the Pauli principle as they fill the available states.

3) A normal mode picture. - Recent studies have investigated the superfluidity of ultracold Fermi gases[31, 32, 33, 34] using a perturbation formalism called symmetry-invariant perturbation theory, SPT. This approach, which is a first-principles, general, many-body method with no adjustable parameters, employs group theory and graphical techniques to solve each perturbation order, in principle exactly, rather than using a basis set or numerical methods. The first-order equation, which is harmonic, has been solved exactly through the determination of the group theoretic normal modes with N as a parameter[35, 36, 37]. The Pauli principle is applied using an adiabatic transition from independent particles to an interacting regime[38, 39] without explicit antisymmetrization of the many-body wave function thus circumventing the intensive numerical work typically required. Despite no explicit real-space two body pairing, first-order results yielded close agreement with experimental data for multiple properties without higher order terms both in the strongly-interacting unitarity regime as well as for weaker interactions from the BCS regime to unitarity[39, 40, 41, 42].

These properties included ground state energies[39], critical temperatures[40], excitation frequencies[40, 43], thermodynamic entropies and energies[40, 41], as well as the compressibility[42] and the lambda transition in the specific heat[41], well known signatures of the onset of superfluidity. These results were obtained with no adjustable parameters and with seconds of desktop computer time due to the use of symmetry in the group theoretic approach and the enforcement of the Pauli principle 'on paper' which avoids the explicit determination of a many-body antisymmetric wave function. (A brief discussion of these results and an explanation of the underlying microscopic basis can be found in Supplemental Information Section I. A-D. in Ref. [44]. For more detail, see Refs. [40, 41, 43].)

These results suggested the possibility that normal modes might offer an alternative microscopic basis for superfluid behavior[44] differing from the conventional view that some fermions form loosely bound pairs that condense into a macroscopic occupation of the lowest state[12, 13, 14, 15, 16, 17, 18, 19, 20, 45, 46, 47, 48, 49]. In addition to producing good agreement with experimental data of multiple properties, normal mode dynamics have suggested an interesting microscopic explanation for the universal behavior at unitarity[43, 50].

Offering an alternative route to a phase coherent macroscopic wave function using normal modes necessarily draws attention to the importance of inter-pair correlations which are due to the Pauli principle and which have always been recognized as crucial to accurately describe superconductivity/superfluidity[51, 52, 53]. Based on these findings, the goal of this study is to understand the roles that the Heisenberg uncertainty principle and the Pauli principle play in producing a superfluid state. This approach will utilize the group theoretic expression for the energy through first order and the restrictions imposed by these two fundamental principles to analyze the effects that combine to produce and support superfluid behavior.

4) Reimagining superfluidity. - The perspective of fermionic superfluidity used in this study of zero-point energy is an extension of previous work that reimagined the microscopic basis of superfluidity[44]. This reimagination adheres closely to the early tenets of superconductivity/superfluidity[54] which assumed two-body pairing solely in momentum space, not in real space, and was used to reinterpret several interrelated phenomena including Cooper pairs, the Fermi sea, and Pauli blocking. The Pauli principle, in its recently revealed role in collective motion, played a critical role in the proposed dynamics selecting the allowed normal modes.

The Pauli principle is known to dominate the inter-pair interactions in the BCS ansatz[51, 52, 53], and is instrumental to producing key properties of superfluidity/superconductivity including an excitation gap, the rigidity of the wave function responsible for the Meissner effect, and the absence of resistance to current flow. It is interesting that early work did not assume two-body pairing in real space. The highly successful BCS theory proposed in 1957[54] assumes the pairing of fermions only in momentum space with $+k$ and $-k$ values. As the 1957 paper states, the BCS wave function describes the "coherence of large numbers of electrons," but does not propose fermion pairs localized into pseudomolecules that transition as in Bose-Einstein condensation[54]. As suggested by London in 1950, a superconductor is a "quantum structure on a macroscopic scale... a kind of solidification or condensation of the

average momentum distribution” of the electrons. “It would not be due to distinct electrons at separate places having the same momentum”, but “it would arise from wave packets of wide extension in space assigning the same local momentum to the entire superconductor” [55]. These early concepts of superfluidity/superconductivity as well as the seminal properties: momentum space pairing, the long-range order over macroscopic distances, the wave function “rigidity”, and the gap in the excitation spectrum [56, 57] are naturally present in a normal mode picture of superfluidity.

In this paper, I will use the formula for the ground state, i.e. zero-point energy of a Fermi gas from the first order SPT solution to analyze the contributions from both the Heisenberg uncertainty principle and the Pauli principle to this energy. Since the Pauli principle has been applied ‘on paper’ through an adiabatic transition to the interacting case, this formula clearly shows the contribution of the Pauli principle to this energy. I will separate out this Pauli contribution and define the remainder as the ‘non-Pauli’ contribution to the zero-point energy, due only to the uncertainty principle i.e. the lowest energy that would be possible if all the particles could reside in the lowest state. I will compare these separate contributions to the corresponding contributions for independent, non-interacting identical fermions in a three dimensional well for which the Pauli principle contribution is, of course, well known. These two fundamental principles will be shown to work together to create a very low energy state with a condensed i.e. squeezed value of the momentum and an extended state in position space. This state lies significantly lower than the next higher normal mode state creating a gap that supports superfluid behavior.

2 Symmetry-Invariant Perturbation Theory: a group theoretic and graphical approach to the general N-body problem

1) **Overview.** - Symmetry-invariant perturbation theory is a non-numerical approach to many-body problems. It uses symmetry rather than intensive numerical methods to describe many-body systems, and thus can offer clear physical insight into the underlying dynamics when higher order terms are small. The perturbation parameter is the inverse dimensionality of space. Originally developed by t’Hooft in quantum chromodynamics [58], and subsequently used by Wilson [59] in condensed matter to calculate critical exponents for $D = 3$ phase transitions starting from the $D = 4$ exact values, $1/D$ or $1/N$ expansions have now been developed to study physical systems in multiple fields of physics from atomic and molecular [60, 61, 62, 63, 64, 65, 66, 67, 68, 69, 70, 71, 72, 73, 74, 75, 76, 77, 78] and condensed matter [59, 79, 80, 81], to quantum field theory [82, 83, 84, 85, 86, 87, 88].

Initially, the SPT formalism was developed to handle the large ultracold ensembles of bosons being studied in atomic physics/condensed matter communities [35, 36, 37, 89, 90, 91, 92]. More recently, it was extended to ultracold Fermi gases [39, 40, 41] which are subject to Pauli constraints [38, 39, 41, 93]. Currently, this method is formulated through first order for three dimensional $L = 0$ systems with spherically-symmetric confinement potentials and general interaction potentials. The SPT approach uses symmetry to tackle the N -scaling problem [35, 36, 37, 94, 95], rearranging the work

required for an exact solution so the exponential scaling depends on the order of the series, not the value of N as is the case in conventional many-body approaches. To take advantage of maximal symmetry, a perturbation series is formulated about a large-dimension structure whose point group is isomorphic to the symmetric group S_N , then evaluated for $D = 3$. This approach enables the extraction of the work at each order that scales exponentially as a pure mathematical problem (cf. the Wigner-Eckart theorem)[96, 97]. In principle, this extracted problem can be solved exactly using group theoretic methods, and saved[98], significantly reducing the numerical cost and underpinning the robustness of this non-numerical approach.

Unlike conventional perturbation approaches, the perturbation in SPT does not involve the strength of the interaction and so it can be applied to strongly interacting systems such as the unitary regime. This many-body approach, however, does not offer a mechanism for the transition to diatomic molecules in the BEC regime. In principle, the BEC regime could be described by including higher-order terms although the number of terms required would probably undermine any physical insight and going to higher order is now exponentially difficult.

Since even the lowest order contains beyond-mean-field effects, excellent first-order results have been obtained[39, 41, 89] as seen in earlier dimensional approaches[65, 99, 100, 101, 102]. The current formalism has been extensively tested on a fully-interacting model problem of harmonically-confined, harmonically-interacting particles[38, 91, 92, 93]. Agreement of ten or more digits was obtained between the SPT wave function and the exact wave function obtained independently verifying this many-body formalism[91] and the analytic forms for the group-theoretic, N -body normal modes.

2) The SPT formalism. - In D dimensional Cartesian coordinates, the N -body Schrödinger equation can be written:

$$H\Psi = \left[\sum_{i=1}^N h_i + \sum_{i=1}^{N-1} \sum_{j=i+1}^N g_{ij} \right] \Psi = E\Psi, \quad (2)$$

$$\begin{aligned} h_i &= -\frac{\hbar^2}{2m_i} \sum_{\nu=1}^D \frac{\partial^2}{\partial x_{i\nu}^2} + V_{\text{conf}} \left(\sqrt{\sum_{\nu=1}^D x_{i\nu}^2} \right), \\ g_{ij} &= V_{\text{int}} \left(\sqrt{\sum_{\nu=1}^D (x_{i\nu} - x_{j\nu})^2} \right), \end{aligned} \quad (3)$$

where h_i represents a single-particle Hamiltonian, V_{int} denotes a general two-body interaction potential, $x_{i\nu}$ refers to the ν^{th} Cartesian component of the i^{th} particle, and V_{conf} is a spherically-symmetric confining potential[35, 36, 37]. The Hamiltonian is transformed to internal coordinates, r_i and γ_{ij} , where $r_i = \sqrt{\sum_{\nu=1}^D x_{i\nu}^2}$, ($1 \leq i \leq N$), are the N D -dimensional scalar radii and $\gamma_{ij} = \cos(\theta_{ij}) = \left(\sum_{\nu=1}^D x_{i\nu} x_{j\nu} \right) / r_i r_j$, ($1 \leq i < j \leq N$), are the $N(N-1)/2$ cosines of the angles between the radial vectors.

The first-order derivatives are removed using a similarity transformation[103], and the large-dimension limit of the Schrödinger equation is regularized by a scale factor. Substituting the scaled variables and defining the perturbation parameter as $\delta = 1/D$

gives:

$$\bar{H}\Phi = (\delta^2\bar{T} + \bar{U} + \bar{V}_{\text{conf}} + \bar{V}_{\text{int}})\Phi = \bar{E}\Phi. \quad (4)$$

$$\begin{aligned} \bar{T} &= \sum_{i=1}^N \left(-\frac{1}{2} \frac{\partial^2}{\partial \bar{r}_i^2} - \frac{1}{2\bar{r}_i^2} \sum_{j \neq i} \sum_{k \neq i} \frac{\partial}{\partial \gamma_{ij}} (\gamma_{jk} - \gamma_{ij}\gamma_{ik}) \frac{\partial}{\partial \gamma_{ik}} \right) \\ \bar{U} &= \sum_{i=1}^N \left(\frac{\delta^2 N(N-2) + (1 - \delta(N+1))^2 \left(\frac{\Gamma^{(i)}}{\Gamma} \right)}{8\bar{r}_i^2} \right) \\ \bar{V}_{\text{conf}} &= \sum_{i=1}^N \frac{1}{2} \bar{r}_i^2, \quad \bar{V}_{\text{int}} = \frac{\bar{V}_0}{1 - 3b'\delta} \sum_{i=1}^{N-1} \sum_{j=i+1}^N 1 - \tanh \Theta_{i,j} \end{aligned}$$

The Gramian determinant Γ contains elements γ_{ij} (see Appendix D in Ref [35]), and the $\Gamma^{(i)}$ determinant excludes the row and column of the i^{th} particle.

Defining $\Theta_{ij} = \frac{c_0}{1-3\delta} \left(\frac{\bar{r}_{ij}}{\sqrt{2}} - \bar{\alpha} - 3\delta(\bar{R} - \bar{\alpha}) \right)$, with $\bar{r}_{ij} = \sqrt{\bar{r}_i^2 + \bar{r}_j^2 - 2\bar{r}_i\bar{r}_j\gamma_{ij}}$ the interatomic separation, \bar{R} the range of the square-well potential, and $\bar{\alpha}$ a constant which softens the potential as $D \rightarrow \infty$, the form of \bar{V}_{int} reduces to a square well at $D = 3$ and is differentiable away from $D = 3$ permitting the dimensional analysis[35, 89]. The constant b' is selected so at unitarity with $\bar{V}_0 = 1.0$, the scattering length is infinite. To reach the weaker interactions of the BCS regime, \bar{V}_0 is scaled to smaller values. The range of the square-well potential $\bar{R} \ll \bar{a}_{ho}$ and is systematically reduced to extrapolate to zero-range interaction.

When $D \rightarrow \infty$, the second derivative terms drop out producing a static problem at zeroth order with an effective potential, \bar{V}_{eff} :

$$\bar{V}_{\text{eff}} = \sum_{i=1}^N \bar{U}(\bar{r}_i; \delta) + \bar{V}_{\text{conf}}(\bar{r}_i; \delta) + \sum_{i=1}^{N-1} \sum_{j=i+1}^N \bar{V}_{\text{int}}(\bar{r}_i, \gamma_{ij}; \delta).$$

The minimum of this effective potential is an infinite-dimensional maximally-symmetric structure with all \bar{r}_i and γ_{ij} equal: for $D \rightarrow \infty$, $\bar{r}_i = \bar{r}_\infty (1 \leq i \leq N)$ and $\gamma_{ij} = \gamma_\infty (1 \leq i < j \leq N)$. Two minimum conditions: $\left. \left(\frac{\partial \bar{V}_{\text{eff}}}{\partial \bar{r}_i} \right) \right|_\infty = 0$, $\left. \left(\frac{\partial \bar{V}_{\text{eff}}}{\partial \gamma_{ij}} \right) \right|_\infty = 0$ yield two equations in \bar{r}_∞ and γ_∞ : $\bar{r}_\infty = \frac{1}{\sqrt{2}\sqrt{1+(N-1)\gamma_\infty}}$ and $\frac{\gamma_\infty(2+(N-2)\gamma_\infty)}{(1-\gamma_\infty)^{3/2}\sqrt{1+(N-1)\gamma_\infty}} + \bar{V}_0 \text{sech}^2(\Theta_\infty) \Theta'_\infty = 0$. Expanding about the minimum $(r_\infty, \gamma_\infty)$: $\bar{r}_i = \bar{r}_\infty + \delta^{1/2} \bar{r}'_i$ and $\gamma_{ij} = \gamma_\infty + \delta^{1/2} \gamma'_{ij}$, sets up a power series in $\delta^{1/2}$.

3) The FG method. - The first-order, $\delta = 1/D$, equation is harmonic and is solved exactly using group theory to obtain the N -body normal modes[35, 36, 37]. The first-order Hamiltonian, \bar{H}_1 , is defined in terms of the constant matrices, \mathbf{F} and \mathbf{G} composed of potential terms and kinetic energy terms respectively, evaluated at the

large dimension limit:

$$\bar{H}_1 = -\frac{1}{2}\partial_{\bar{y}'}^T \mathbf{G} \partial_{\bar{y}'} + \frac{1}{2}\bar{\mathbf{y}}'^T \mathbf{F} \bar{\mathbf{y}}' + v_o, \quad (5)$$

with v_o a constant[35]. The FG matrix method[104], extensively used in molecular physics, is utilized to obtain the normal-mode frequencies[35] and coordinates[36]. (Appendix A in Ref. [35] contains a brief summary.) Only five distinct frequencies, $\bar{\omega}$, are obtained regardless of the value of N . This large degeneracy reflects the very high degree of symmetry in the \mathbf{F} and \mathbf{G} matrices which are evaluated for the $D \rightarrow \infty$, maximally-symmetric structure which has a single value for all \bar{r}_∞ and γ_∞ . These matrices are thus invariant under the $N!$ particle interchanges of S_N and do not connect subspaces belonging to different irreducible representations (irreps) of S_N [105, 106]. Consequently, the normal coordinates transform under irreps of S_N .

The five irreps include: a one-dimensional radial and a one-dimensional angular irrep both labelled by the partition $[N]$, an $N - 1$ -dimensional radial and an $N - 1$ -dimensional angular irrep both labelled by the partition $[N - 1, 1]$, and an angular irrep of dimension $N(N - 3)/2$ labelled by $[N - 2, 2]$. These irreps are denoted by shorthand labels: $\mathbf{0}^-$, $\mathbf{0}^+$, $\mathbf{1}^-$, $\mathbf{1}^+$, and $\mathbf{2}$ respectively, (see Refs. [36, 37]). The character of these five modes has been analyzed as a function of N in Ref. [50]. For N large, the single normal mode of type $\mathbf{0}^+$ has center of mass motion; the single $\mathbf{0}^-$ mode is a breathing motion; the $N - 1$ type $\mathbf{1}^+$ modes exhibit particle-hole/single-particle angular excitation behavior; the $N - 1$ type $\mathbf{1}^-$ modes display particle-hole i.e. single-particle radial excitation behavior; and the $N(N - 3)/2$ type $\mathbf{2}$ modes correspond to phonon compressional modes.

A symmetry coordinate vector, S , is defined:

$$\mathbf{S} = \begin{pmatrix} \mathbf{S}_{\bar{r}'}^{[N]} \\ \mathbf{S}_{\bar{\gamma}'}^{[N]} \\ \mathbf{S}_{\bar{r}'}^{[N-1, 1]} \\ \mathbf{S}_{\bar{\gamma}'}^{[N-1, 1]} \\ \mathbf{S}_{\bar{\gamma}'}^{[N-2, 2]} \end{pmatrix} = \begin{pmatrix} W_{\bar{r}'}^{[N]} \bar{r}' \\ W_{\bar{\gamma}'}^{[N]} \bar{\gamma}' \\ W_{\bar{r}'}^{[N-1, 1]} \bar{r}' \\ W_{\bar{\gamma}'}^{[N-1, 1]} \bar{\gamma}' \\ W_{\bar{\gamma}'}^{[N-2, 2]} \bar{\gamma}' \end{pmatrix}, \quad (6)$$

where $W_{\bar{r}'}^{[\alpha]}$ and $W_{\bar{\gamma}'}^{[\alpha]}$ are transformation matrices determined using the theory of group characters to decompose \bar{r}' and $\bar{\gamma}'$ into basis functions that transform under the five irreps of S_N [36]. The \mathbf{FG} method is applied to determine the normal modes. In the $[N]$ and $[N - 1, 1]$ sectors, the normal coordinates have mixed radial and angular behavior. The $[N - 2, 2]$ normal modes are purely angular due to the absence of \bar{r}' symmetry coordinates. The amount of radial/angular mixing is dependent on the first-order Hamiltonian terms.

4) **The energy.** - The energy through first-order in $\delta = 1/D$ [35, 65]:

$$\bar{E} = \bar{E}_\infty + \delta \left[\sum_{\mu=\{\mathbf{0}^\pm, \mathbf{1}^\pm, \mathbf{2}\}} (n_\mu + \frac{1}{2}d_\mu)\bar{\omega}_\mu + v_o \right], \quad (7)$$

has the form of a harmonic energy in terms of the normal mode frequencies, where \bar{E}_∞ denotes the energy at the minimum of $\bar{V}_{\text{eff}}|_\infty$, μ labels the five types of normal modes (irrespective of the value of N , see Ref. [35] and Ref.[15] in [36]), with n_μ representing the total normal mode quanta with frequency $\bar{\omega}_\mu$; and v_o is a constant (defined in Ref. [35], Eq.(125)). The five roots have multiplicities: $d_{\mathbf{0}^+} = 1, d_{\mathbf{0}^-} = 1, d_{\mathbf{1}^+} = N - 1, d_{\mathbf{1}^-} = N - 1, d_{\mathbf{2}} = N(N - 3)/2$.

5) The Pauli principle. - Eq. (7) defines the ground state/zero-point energy as well as the excited state spectrum by assigning normal mode quantum numbers consistent with the Pauli principle. The allowed assignments are determined by finding a correspondence between the normal mode states $|n_{\mathbf{0}^+}, n_{\mathbf{0}^-}, n_{\mathbf{1}^+}, n_{\mathbf{1}^-}, n_{\mathbf{2}} \rangle$ and the non-interacting states of the three dimensional harmonic oscillator ($V_{\text{conf}}(r_i) = \frac{1}{2}m\omega_{ho}^2 r_i^2$) whose restrictions due to antisymmetry are well known. In the double limit, $D \rightarrow \infty, \omega_{ho} \rightarrow \infty$, both representations are valid, so the quantum numbers can be related. The radial and angular characters separate resulting in two conditions[38, 39]:

$$2n_{\mathbf{0}^-} + 2n_{\mathbf{1}^-} = \sum_{i=1}^N 2\nu_i, \quad 2n_{\mathbf{0}^+} + 2n_{\mathbf{1}^+} + 2n_{\mathbf{2}} = \sum_{i=1}^N l_i, \quad (8)$$

with ν_i and l_i the radial and orbital angular momentum quantum numbers respectively of the three dimensional oscillator, and $n_i = 2\nu_i + l_i$ the i th particle energy level quanta defined by: $E = \sum_{i=1}^N [n_i + \frac{3}{2}] \hbar\omega_{ho} = \sum_{i=1}^N [(2\nu_i + l_i) + \frac{3}{2}] \hbar\omega_{ho}$. This strategy is analogous to Landau's use of the non-interacting system in Fermi liquid theory to set up the correct Fermi statistics as interactions evolve adiabatically[107].

For ultracold systems, only the lowest angular and radial modes will be occupied i.e. phonon, $n_{\mathbf{2}}$, and single-particle radial excitation modes, $n_{\mathbf{1}^-}$, yielding:

$$2n_{\mathbf{1}^-} = \sum_{i=1}^N 2\nu_i, \quad 2n_{\mathbf{2}} = \sum_{i=1}^N l_i. \quad (9)$$

Near $T = 0$, the system energy becomes too small to excite a radial mode, so only phonon modes are excited creating a gap that supports superfluid behavior.

3 Zero-point energy considerations

1) The ground state energy. - The SPT ground state energy that will be used to analyze the contributions from the uncertainty principle and the Pauli principle has been previously calculated and compared to results in the literature both at unitarity[39] and across the BCS to unitarity transition[40]. In Fig. A1 in the Appendix, we reproduce a figure from Ref. [39] which shows the excellent agreement at unitarity with benchmark Monte Carlo calculations reported for values of $N \leq 30$ [108]. Fig. A2 in the Appendix is taken from Ref. [40] and shows energies across the BCS to unitarity transition with similarly good agreement of the SPT results with both experiment and theory.

The formula for the energy, Eq. 7, shows explicitly the contribution of the Pauli principle in the quanta, $n_{0+}, n_{0-}, n_{1+}, n_{1-}, n_2$ included in the sum over the five frequencies, $\bar{\omega}_\mu$. For temperatures near $T = 0$, only phonon modes are occupied so only n_2 is nonzero. Its value is obtained as explained above using an adiabatic transition from the independent particle case for which the restrictions of the Pauli principle are well known to the interacting case. Knowing the value of n_2 , the contribution of the Pauli principle can be subtracted from the total energy to leave a non-Pauli contribution due only to the uncertainty principle, i.e., the lowest energy that would be possible if the particles could all reside in the same lowest state. The contributing terms include \bar{E}_∞ , the energy at the minimum of the effective potential which includes effects from the trap as well as from the interactions of the N fermions, as well as the sum over the multiplicities for each frequency and a correction term, v_o . (For the formula for \bar{E}_∞ see Eq. 116 in Ref. [35].)

2) The Fermi sea. - While the implications of the Heisenberg uncertainty principle apply equally to bosons and fermions, systems of bosons are not subject to the Pauli principle. Thus once a lowest single particle state is determined that satisfies the Heisenberg uncertainty principle for one of the bosons, all of the bosons can occupy this state. For fermions, only one fermion (or two fermions of opposite spin) can occupy the lowest spatial state that satisfies the uncertainty principle. This results in the concept of a Fermi sea where degenerate fermions fill all the lowest allowed energy levels according to the Pauli principle. From an independent particle view, degenerate Fermi systems have all the lowest energy states filled, with a “Fermi surface” dividing the filled from the unfilled levels. This “sea” of fermions in energy space is defined by the Fermi energy, the largest occupied energy in the system. The Fermi sea Pauli-blocks states below the Fermi energy, thus the Pauli principle controls the behavior of these degenerate systems, suppressing processes that require an unfilled level in the Fermi sea. Such behavior has been observed in the lab[109, 110, 111]. Degeneracy pressure, a striking feature of these systems, is due to the Pauli principle requiring the occupation of high energy levels and is responsible for the stability of degenerate Fermi systems and thus their prevalence in our universe.

From a collective viewpoint, the concept of a Fermi sea is defined in terms of the lowest occupied phonon normal mode allowed by the Pauli principle. The occupations of the states in the independent particle picture dictate the restriction on the minimum number of quanta required in the collective motion of the ensemble. For ultracold systems at $T = 0$, only phonon modes are occupied so the Fermi sea of occupied independent energy states becomes an energy minimum of the phonon collective mode, with lower energy phonon modes unoccupied, i.e. Pauli-blocked from occupation. From the independent particle view, the Fermi energy is the energy of the highest occupied independent energy state, while in the collective view, the Fermi energy is the energy of the lowest occupied phonon mode. The quantum numbers in these two regimes are discussed in the Supplemental Information, Section I.E. in Ref. [44].

3) The evolution from independent particles to the strongly correlated unitary regime. - It is helpful to imagine the evolution from the independent particle picture to the strongly interacting regime at unitarity. This transition has been studied previously using the SPT approach for the five normal mode frequencies as a function of

both particle number, N , and interaction strength[43]. As the particles begin to interact, the Hamiltonian governing the behavior of the particles now includes this new interaction potential term. The independent particles that were responding only to the trap begin to interact with every other particle in this N -body ensemble evolving into highly-correlated, collective behavior. In the SPT formalism, these interactions combine with the harmonic trap term to produce first-order solutions which are normal modes of motion. The familiar evenly-spaced three dimensional harmonic spectrum of the trapped independent particles with frequency ω_{ho} evolves to a new set of spectra that reflect the interacting particles. These new spectra are composed of the normal mode frequencies, five different frequencies that correspond to the five irreducible representations under which the normal modes transform. In Fig. A3 in the Appendix, I reproduce three figures from Ref. [43] showing the evolution of these five frequencies across the BCS to unitarity transition for three increasing ensemble sizes. These five frequencies define five separate, evenly-spaced spectra. The lowest frequency, ω_2 , belonging to the $[N - 2, 2]$ irreducible representation corresponds to phonon or compressional motion which is a completely angular mode that transitions adiabatically to angular states of the independent particle regime. At temperatures near absolute zero, these compressional modes are the only ones occupied with the actual occupation dictated by the Pauli principle and the degeneracies of this three dimensional many-body system. The particles in a phonon mode are moving in sync with a single frequency and phase, and thus this N -body wave function has a large spatial expanse. Near $T = 0$, the individual particles are no longer identifiable due to their large overlapping de Broglie wavelengths yielding a large uncertainty in the position of each particle. Due to this large uncertainty in position, the average momentum of the N particles is allowed by the uncertainty principle to condense toward a single, very small, absolute value, $|k|$. As the particles move back and forth in lockstep, from $+k$ to $-k$, the uncertainty in the momentum is squeezed to $2|k|$.

It is instructive to compare the different contributions from the uncertainty principle alone and from the Pauli principle to the zero-point energy in these two regimes: the independent particle regime and the strongly interacting unitarity regime. This evolution can also be viewed as evolving from the weakly interacting BCS regime with infinitesimally small particle interactions, i.e. with the particles responding essentially only to the trap, to the strongly-interacting, strongly-correlated unitary regime. This is achieved in the laboratory in cold fermion experiments using a Feshbach resonance to tune the particle interactions. In the following discussions, I will assume a spin-balanced ensemble of identical fermions as is typical in these cold atom experiments.

Fig. 1 compares the total zero-point energies in these two regimes as a function of N for $5 \leq N \leq 30$. As expected from the difference in the spacing of the spectra for each regime, i.e. $\omega_2 \ll \omega_{ho}$, the independent particle zero-point energies for an N -body system of identical fermions in an harmonic trap are significantly higher than the zero-point energies for the strongly interacting unitary regime with the difference increasing as N increases. (This difference can also be verified in Fig. A2 in the Appendix which shows the ground state/zero-point energy decreasing across the BCS to unitarity transition.) Clearly, the effect of the Pauli principle for these two

systems of identical fermions is greater for the system with the more widely spaced spectrum of energy levels (independent particles with ω_{ho}) that become successively occupied as the fermions fill all the lower levels.

In Fig. 2, the contribution from the Pauli principle is separated out from the total zero-point energy for the independent particles leaving the contribution due only to the uncertainty principle. As one can see for this regime, the effect of the Pauli principle on the zero point energy starts out below the uncertainty principle (non-Pauli) contribution, but quickly becomes the larger contribution with a steeper slope as N increases.

Fig. 3 shows a similar breakdown for the zero-point energy in the strongly interacting unitary regime. Here the small spacing (ω_2) of the spectrum results in a much smaller contribution from the Pauli principle. The remaining contribution from the uncertainty principle makes up the overwhelming majority of the total zero-point energy.

Figs. 4-6 show contributions *per particle* for much higher values of N , $N \leq 5000$. Fig. 4 compares the total zero-point energies per particle in these two regimes. As expected the independent particle zero-point energies are significantly higher per particle than the zero-point energies per particle for the strongly interacting unitary regime with the difference increasing as N increases.

Analyzing the different contributions in the independent particle regime for these larger values of N , Fig. 5 shows that the Pauli principle is responsible for the overwhelming amount of the total zero-point energy, tracking close to the total while the contribution from the uncertainty principle per particle stays the same for all N at $3/2 \hbar\omega_{ho}$ as expected.

The opposite is true for the interacting regime at unitarity as shown in Fig. 6. The contribution per particle from the Pauli principle effect remains quite small, increasing very slightly with N , leaving the majority of the zero-point energy per particle contributed by the non-Pauli terms which are due to the uncertainty principle and closely track the total zero-point energy.

Comparing the two graphs, Figs. 5 and 6, (note the different scales on the vertical axis), the contributions from the Pauli principle and the uncertainty principle, i.e. the non-Pauli terms, seem to trade places. In the unitary regime with interacting particles, we see that the non-Pauli contributions per particle to the zero-point energy are larger and increase with N , while the Pauli contributions are much smaller compared to the independent particle regime. In contrast, the Pauli principle dominates in the independent particle regime, while the non-Pauli uncertainty principle contributions are constant at $3\hbar\omega/2$ as expected. This change, of course, takes place across the BCS to unitarity transition and is due to the increase in inter-particle interactions that occurs as strong correlations set up collective behavior. These interactions increase the contribution to the zero-point energy from the uncertainty principle alone and suppress the contributions from the Pauli principle as the spectrum is squeezed, in effect exchanging the importance of the effects from these two fundamental principles. Due to the larger reduction in the Pauli contribution, the net effect is a lower zero-point energy for the interacting system as confirmed experimentally.

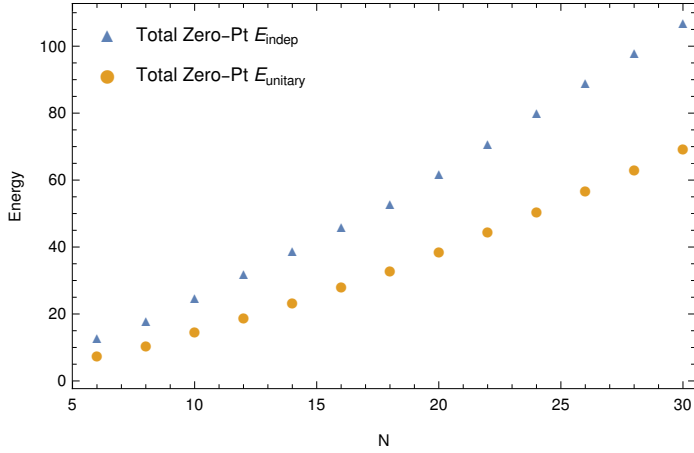


Fig. 1: Comparison of the SPT zero-point/ground state energies for the independent particle case and the unitarity regime as a function of N in units of $\hbar\omega_{ho}$.

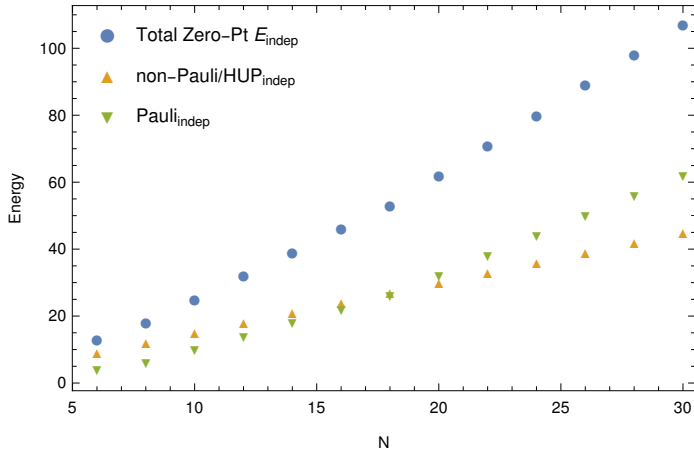


Fig. 2: The independent particle ground state/zero-point energies with the separate contributions from the Pauli principle and the non-Pauli terms as a function of N in units of $\hbar\omega_{ho}$.

4 Discussion

The difference in the zero-point energy between the independent particle regime and the strongly interacting unitary regime near $T = 0$ is due to several factors that work in concert. As noted above, I will assume a spin-balanced ensemble of identical fermions as are used in most ultracold experiments with atomic fermions.

1) **Squeezing the Heisenberg uncertainty principle.** - In the independent particle regime where the particles are responding only to a harmonic trap, the spectrum is spaced by $\hbar\omega_{ho}$ and the uncertainty principle is saturated for the lowest state which

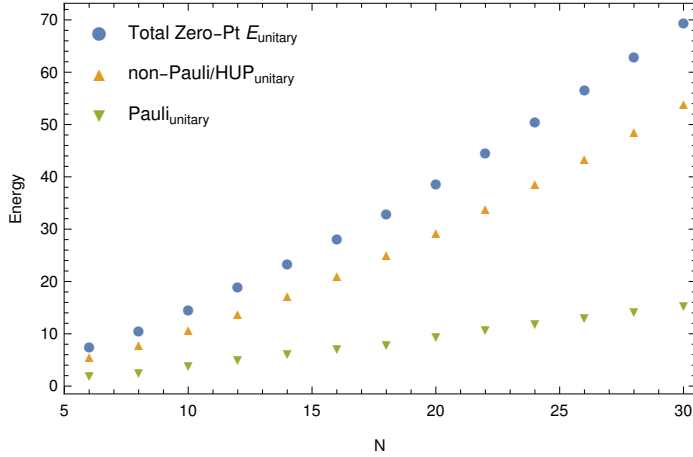


Fig. 3: The SPT ground state/zero-point energies at unitarity with the contributions from the Pauli and the non-Pauli terms as a function of N in units of $\hbar\omega_{ho}$.

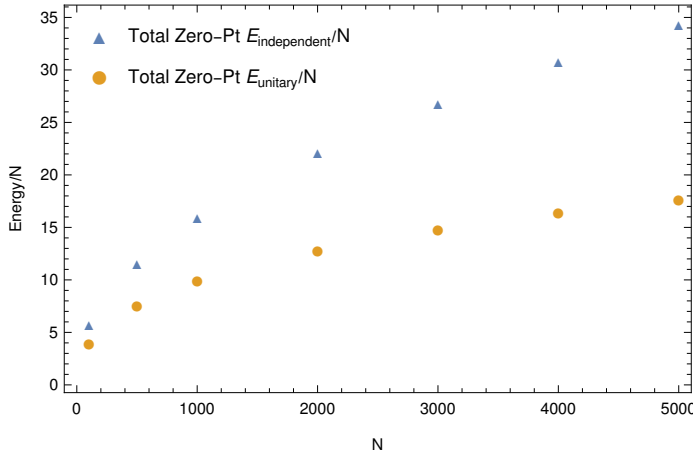


Fig. 4: Comparison of the SPT zero-point energies per particle for the independent particle case and the unitarity regime as a function of N for large values of N in units of $\hbar\omega_{ho}$.

is occupied by a pair of fermions with equal uncertainties in position and momentum. As higher and higher states fill with fermions, the Pauli principle has a larger and larger effect dominating the zero-point energy as N increases.

In contrast, the interacting unitarity regime satisfies the uncertainty principle with a large uncertainty in position and a very small uncertainty in the momentum. To achieve such a small value of the momentum requires the expansion of the uncertainty in position space so the Heisenberg uncertainty principle, whose lower bound was saturated in the lowest state in the independent particle regime, continues to be

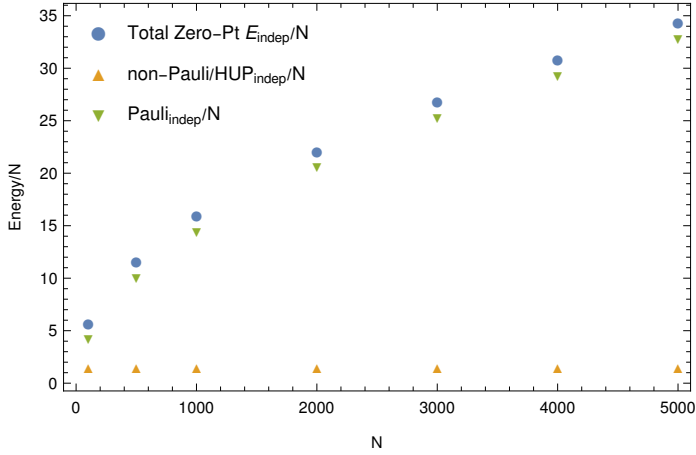


Fig. 5: The independent particle ground state/zero-point energies per particle with the contributions from the Pauli principle and the non-Pauli terms as a function of N in units of $\hbar\omega_{ho}$.

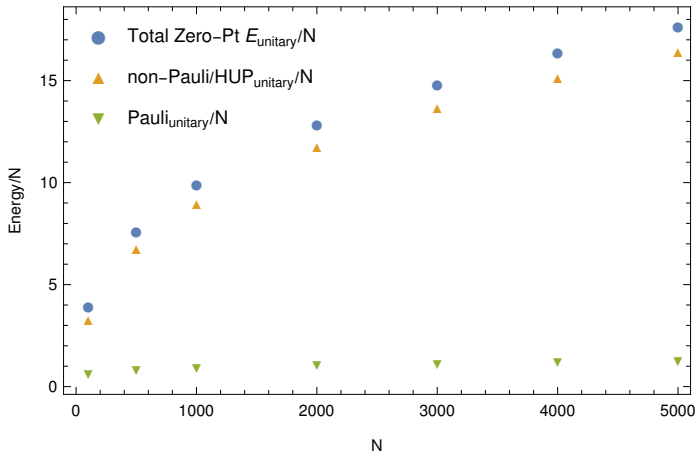


Fig. 6: The SPT ground state/zero-point energies per particle at unitarity with the contributions from the Pauli principle and the non-Pauli terms as a function of N in units of $\hbar\omega_{ho}$.

satisfied. This is achieved by the emergence of highly-correlated, collective motion of the fermions near $T = 0$ and the overlapping of their de Broglie wavelengths yielding a large uncertainty in the position since the particles can no longer be distinguished individually. The phonon normal mode state near $T = 0$ with all the particles moving in lockstep produces this dynamic. The ground state energy of this system has been calculated through first order in the SPT perturbation series using Eq. 7 which shows several terms contributing to the zero-point energy from the uncertainty principle as

well as a contribution from the Pauli principle from the term that sums over the normal mode quantum numbers $n_{\mathbf{0}^+}, n_{\mathbf{0}^-}, n_{\mathbf{1}^+}, n_{\mathbf{1}^-}, n_2$. This ground state energy agrees well with both experiment and other theoretical work. See Figs. A1 and A2 in the Appendix. (In Eq. 7, the term, $+\frac{1}{2}d_\mu\bar{\omega}_\mu$ in the sum over the normal modes:

$$\sum_{\mu=\mathbf{0}^\pm, \mathbf{1}^\pm, \mathbf{2}} (n_\mu + \frac{1}{2}d_\mu)\bar{\omega}_\mu \quad (10)$$

appears at first glance to be the zero-point energy of this normal mode system. However, the perturbation derivation for the ground state energy includes a zeroth order term, E_∞ and a correction term v_o that must be included to give the correct contribution.)

The squeezed value of the momentum yields not only a very low energy ground state, but an entire spectrum of squeezed states for these compressional phonon modes. The squeezed spacing, $\hbar\omega_2$, is much smaller than the spacing of the independent particle spectrum, $\hbar\omega_{ho}$.

2) Suppressing the Pauli principle. - Since the value of ω_2 is so small, $\omega_2 \ll \omega_{ho}$, the Pauli contribution, $n_2\hbar\omega_2$ where n_2 is the quantum number of the lowest allowed phonon mode, will be quite small for the typical condensate sizes in experiments compared to the rest of the zero-point energy. This keeps the zero-point energy low, well below the next higher normal mode state, thus setting up a gap that supports superfluid behavior.

As N increases, i.e. as the ensemble size increases, the value of ω_2 decreases as shown in Fig. 7 so the energy levels being filled according to the Pauli principle are merging closer and closer in energy. It is interesting to consider the large N limit where ω_2 limits to zero (see Appendix G in Ref. [43]) so the energy levels are infinitesimally close both to each other and to the lowest phonon level. This means that the fermions can obey the Pauli principle while occupying states essentially in the same energy level and infinitesimally close to the lowest allowed phonon mode, the mode that would be occupied if the particles didn't need to obey the Pauli principle. Unlike degenerate, independent fermions in a harmonic well which fill higher energy states with frequencies increasing by integer multiples of $\hbar\omega_{ho}$, the phonon collective motion at these low temperatures allows the fermions to occupy energy states that are essentially in the same energy level, i.e. behaving in this regard as condensed bosons would, thus circumventing this effect of the Pauli principle completely. (Of course, the fermions in these degenerate or nearly degenerate states are spread out in different wave functions as required by the Pauli principle in contrast to the case of N bosons which can all be in the same ground state wave function resulting in different N -body wave functions for these two systems which could affect other properties and the overall dynamics.)

Fig. 7 shows the very small SPT values for ω_2 for large values of N demonstrating the closeness of the different phonon levels as this spectrum is squeezed. Note that the decrease in ω_2 implies a corresponding decrease in the momentum for these particles which are moving with the same frequency and displacement. (See Section C in the Supplementary Information in Ref. [44].) Correspondingly, there is an increase in the size of the system as N increases which implies an increase in the uncertainty in the position of each particle as required by the uncertainty principle. Thus, Fig. 7 verifies

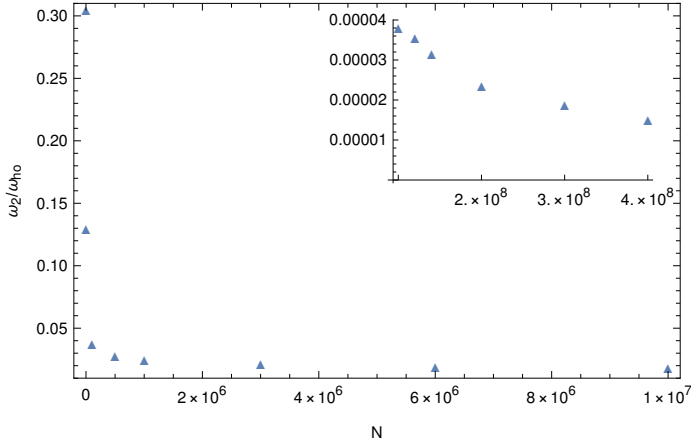


Fig. 7: The SPT phonon normal mode frequency, ω_2 as a function of particle number N . The inset extends to very low values of ω_2 as N reaches values of 10^8

the expected response of complimentary variables obeying the Heisenberg uncertainty principle at the lower bound of this fundamental principle.

3) Manifesting the wave nature of matter. - In item 2) above, I describe an interesting phenomenon in which this effect of the Pauli principle is suppressed and eventually becomes completely circumvented for N very large resulting in an ensemble of identical fermions behaving like identical bosons as they occupy merged energy levels. This suppression of the Pauli principle is due to the squeezed spacing of the phonon spectrum and facilitates the creation of a gap between the fermions in this lowest normal phonon mode and the next higher normal mode. To achieve this extremely small spacing required a large increase in the uncertainty of the position of each particle. This, at first, might seem difficult to imagine at these ultralow temperatures when the particles are moving so slowly. The naive view would be that the particles' position uncertainties at these cold temperatures and slow movements would also be quite small as they make tiny compressional movements. However, as we have seen, the wave nature of the particles becomes manifest due to both the large de Broglie wavelengths near $T = 0$, but also due to the collective motion of the particles controlling the size and phase of the movements. In the large N limit, the fermions begin to occupy infinitesimally close energy levels as the energy states merge into the lowest state and a coherent wave function emerges manifesting macroscopically the wave nature of matter.

4) Engineering the suppression of the Pauli principle. - One can imagine a second possible way to achieve a suppression of this effect of the Pauli principle which does not require these ultralow temperatures. This strategy would involve engineering a system in which the degeneracy (or near degeneracy) of the lowest state(s) is greatly enlarged so that many fermions can reside at the same (or very close) energy as bosons do. This would require the construction of a system with this degeneracy built into the confinement of the particles or the particle interactions or both in order to produce highly degenerate states. In the current case, the degeneracies are constant as the

system transitions adiabatically from the independent particle regime, for which the degeneracies are well known, to the strongly interacting unitary regime (See Section IV in Ref. [38]) so this proposed strategy of circumventing the Pauli principle is not relevant to the present study, but could be an interesting possibility to construct useful gaps in other spectrums of interest.

Note, that these two strategies to suppress the Pauli principle are distinct from the phenomenon of Pauli blocking where the Pauli principle suppresses other processes that need an unfilled state below the Fermi surface. For a degenerate fermionic ensemble these interactions are called 'Fermi blocked' by the filled Fermi sea[109, 110, 111, 112].

5 Conclusions

Understanding the concept of zero-point energy has been a longstanding goal in multiple fields of physics since the advent of quantum mechanics. This fundamental concept representing perhaps the simplest manifestation of the wave nature of matter affects diverse phenomena in our universe and is an active area of research in many areas including the rate of cosmic expansion[1], a possible source of dark energy[1], collective fluctuations of complex molecules[6] and ultracold atoms[113, 114], nanocrystals[7], optomechanical systems[8, 9], and quantum entanglement[115] among other studies.

In this paper, I have investigated the zero-point energy of an ultracold Fermi gas using the formula for the ground state energy from the SPT formalism to separate out the effect of the Pauli principle from the role of the Heisenberg uncertainty principle. The Pauli principle's role in collective motion was previously used to reimagine and reinterpret some of the seminal concepts of superfluidity. Now this collective behavior is studied to understand how the wave-like nature of identical fermions at ultracold temperatures becomes manifest and results in a squeezed spectrum of closely spaced energy levels that supports the emergence of superfluid behavior. The perturbation method employed to analyze these results, SPT, is solved exactly at first order using group theory to yield normal modes obtaining a detailed microscopic view of the underlying dynamics.

The factors that combine to produce the dynamics to support superfluid behavior include: 1) many-body interactions giving rise to strongly correlated, lockstep, collective motion; 2) ultracold temperatures producing large overlapping de Broglie wave lengths that create large uncertainties in the position of each fermion; and finally, 3) the squeezed or condensed value of the momentum of each particle that allows this effect of the Pauli principle to be strongly suppressed as the fermions occupy infinitesimally close states near the lowest energy state.

The effects of these two fundamental principles are well known in the independent particle regime, but, as we have seen, they produce drastically different effects as the particles begin to interact in this ultracold regime. This new dynamic allows the N-body system of identical fermions to converge toward condensed energy levels at this low temperature adopting superfluid behavior which is approaching closer and closer microscopically to bosonic superfluidity.

This collective perspective previously offered an explanation for universal behavior in the unitary regime. The absence of interparticle interactions typically defines a regime of independent particles, but can also be the defining characteristic of a strongly correlated ensemble with particles moving in lockstep with fixed interparticle distances, i.e. angular normal modes. Both types of ensembles are independent of the microscopic details despite having very different underlying dynamics.

Analyzing the zero-point energy from a collective perspective has revealed interesting roles of the Heisenberg uncertainty principle and the Pauli principle working in concert microscopically at these ultracold temperatures to create a superfluid, a powerful macroscopic manifestation of the wave nature of matter.

Declarations

- Funding

This research did not receive funding.

- Competing interests

No, I declare that the author has no competing interests as defined by Springer, or other interests that might be perceived to influence the results and/or discussion reported in this paper. The author has no relevant financial or non-financial interests to disclose.

- Compliance with Ethical Standards

The author has no potential conflicts of interest.

- Consent for publication

All of the material is owned by the author and/or no permissions are required.

- Data Availability

The data generated or analysed during this study are available from the author on reasonable request.

- Code Availability

Not applicable

- Authors' contributions

D.K. Watson, as the sole author, was responsible for the design of this research, the investigation, writing the original draft of the manuscript and editing the final draft.

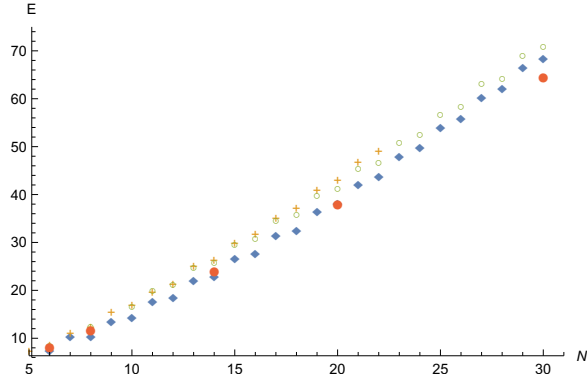


Fig. A1: Ground state energies of the harmonically trapped unitary Fermi gas (units $\hbar\omega_{ho} = 1$). My SPT first-order perturbation results[39] (filled diamonds) are compared to GFMC (+’s)[116], fixed-node DMC (open circles) from Ref. [117], and AFMC results (filled circles, $N=6, 8, 14, 20, 30$ only)[108].

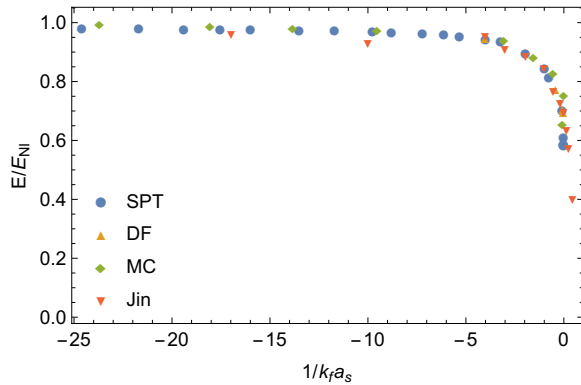


Fig. A2: Ground state energies from BCS to unitarity as a function of $1/k_f a_s$. My SPT results are for $N = 12$ [40] and are compared to experimental [118], density functional (DF)[119] and variational Monte Carlo results (MC)[120].

A The ground state of an ultracold Fermi gas.

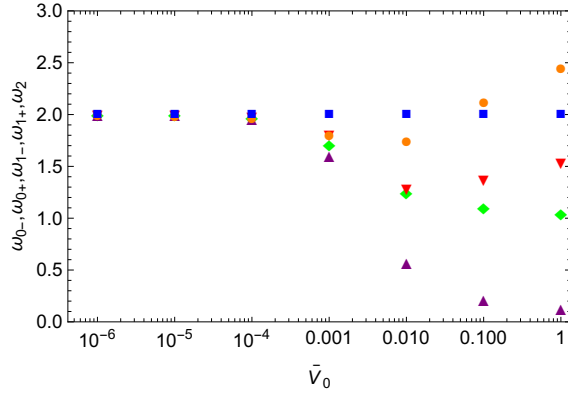
The ground state energy of an ultracold Fermi gas has previously been calculated using the SPT formalism and compared to other theoretical studies including benchmark Monte Carlo results. Fig. A1 below is taken from Ref. [39] and shows the excellent agreement between SPT results and the benchmark results for values of N reported up to 30[108, 116, 117].

Fig. A2 is taken from Ref. [40] and shows the comparison of the SPT ground state energies from the BCS regime of weak interactions to the unitary regime, comparing closely with both experimental and theoretical work in the literature[118, 119, 120].

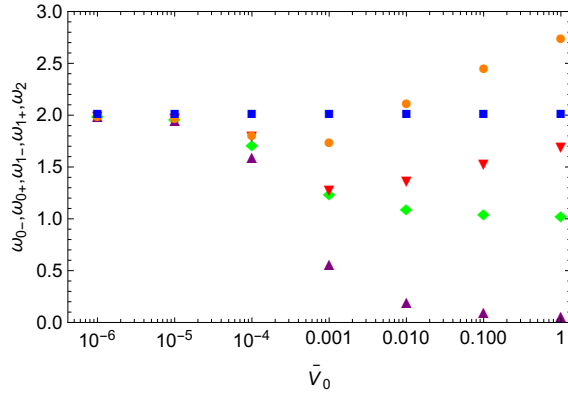
In Fig. A3, I reproduce three figures from Ref. [43] showing the behavior of the five normal mode frequencies across the transition from the non-interacting regime to the

strongly-interacting unitary regime for three different sizes of the ensemble. One can see that the angular frequencies converge to integer multiples of the trap frequency, ω_{ho} , with the phonon frequency limiting to 'zero' times ω_{ho} . See Section VI. D. in Ref. [43] for a discussion of the microscopic dynamics underlying this behavior and Appendix E in Ref. [43] for the derivation of this limiting behavior for the phonon mode.

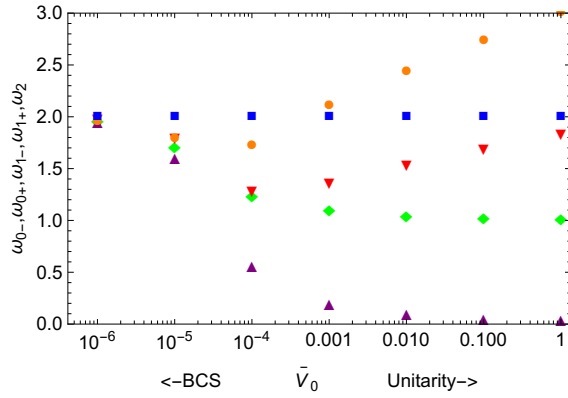
From these three graphs, one can see that as N increases and thus the spatial expanse of the wave function increases yielding a larger uncertainty in the position of each particle, ω_2 decreases implying a decrease in the uncertainty in the momentum as allowed by the uncertainty principle. The phonon states filling with fermions merge closer and closer together so the effect of the Pauli principle continues to be minimized retaining the gap to higher normal modes which supports superfluidity.



(a) a. $N = 10^3$ fermions.



(b) b. $N = 10^4$ fermions.



(c) c. $N = 10^5$ fermions.

Fig. A3: SPT frequencies as a function of the interparticle interaction strength, \bar{V}_0 , from BCS to unitarity in units of the trap frequency from Ref [43]. (ω_{0-} orange dots; ω_{0+} blue squares; ω_{1-} red 'down' triangles; ω_{1+} green diamonds; ω_2 purple 'up' triangles). Note the log scale on the x axis.

References

- [1] M. Maggiore, Phys. Rev. D **83**, 063514 (2011).
- [2] B. Zumino, Nucl. Phys. B **89**, 535 (1975).
- [3] H. B. Nielsen, S. Pallua, and P. Prester, Int. J. Mod. Phys. A **17**, No. 15, 2073 (2002).
- [4] P.W. Milonni, “Zero-Point Energy” in “Compendium of Quantum Physics: Concepts, Experiments, History and Philosophy” edit. by D. Greenberger, K. Hentshel, and F. Weinent; Berlin, Heidelberg, Springer, pp. 864-866 (2009).
- [5] B. Lehnert, AIP Conf. Proc. **1445**, 102 (2012).
- [6] B. Richard et al., Science **389**, 650 (2025).
- [7] R.Duan et al., Phys. Rev. Lett. **135**, 196901(2025).
- [8] F. Lecocq, J.D. Teufel, J. Aumentado and R.W. Simmonds, Nature Physics, **11**, 635 (2015).
- [9] M. Chegnizadeh, M. Scigliuzzo, A. Youssefi, S. Kono, E. Guovskii, T.J. Kippenberg, Science **386**, 1383 (2024).
- [10] I. Errea et al., Nature **578**, 66 (2020).
- [11] B. Setterfield, J Phy Opt Sci, ISSN:2754-4753 (2023).
- [12] G.B. Partridge et al., Phys. Rev. Lett. **95**, 020404 (2005).
- [13] M. Greiner et al., Nature **426**, 537(2003).
- [14] M.W. Zwierlein et. al., Phys. Rev. Lett. **91**, 250401 (2003).
- [15] S. Jochim et al., Science **302**, 2101 (2003).
- [16] J. Kinast et al., Phys. Rev. Lett. **92**, 150402 (2004).
- [17] T. Bourdel et. al., Phys. Rev. Lett. **93**, 050401 (2004).
- [18] C.A. Regal et al., Phys. Rev. Lett. **92**, 040403(2004).
- [19] M.W. Zwierlein et. al., Phys. Rev. Lett. **92**, 120403 (2004).
- [20] C. Chin et al., Science **305**, 1128 (2004).
- [21] C. M. Caves, Phys. Rev. D **23**, 1693 (1981).
- [22] N. Bigelow, Nature **409**, 27 (2001).
- [23] P. Grangier, R.E. Slusher, B. Yurke, and A. LaPorta, Phys. Rev. Lett. **59**. 2153 (1987).
- [24] F. Gerbier, S. Fölling, A. Widera, O. Mandel, and I. Bloch, Phys. Rev. Lett. **96**, 090401 (2006).
- [25] M-Z Huang, J.A. de la Paz, T. Mazzoni,, K. Ott, P. Rosenbusch, A. Sinatra, C.L G. Alzar, and J. Reichel, Phys. Rev. X Quantum, **4**, 020322 (2023).
- [26] R.J. Fletcher, A. Shaffer, C. C. Wilson, P.B. Patel, Z. Yan, V. Crépel, B. Mukherjee, M. Zwierlein, Science **372**, 1318 (2021).
- [27] J.A. Hines, S.V. Rajagopal, G.L. Moreau, M.D. Wahrman, N.A. Lewis, O. Marković, and M. Schleier-Smith, Phys. Rev. Lett. **131**. 063401 (2023).
- [28] J.M. Robinson, M. Miklos, Y.M. Tso, C.J. Kennedy, T. Bothwell, D. Kedar, J.K. Thompson and J. Ye, Nature Physics **20**, 208213 (2024).
- [29] J. Abadie et al., Nat. Phys. **7**, 962(2011).
- [30] J. Aasi et al., Nat. Photon. **7** 613(2013).
- [31] M. Inguscio, W. Ketterle, C. Salomon, Ultracold Fermi Gases, *Proceedings of the International School of Physics Enrico Fermi, Course CLXIV, Varenna* (2006).
- [32] M. Randeria and E. Taylor, Ann. Rev. Condensed Matter Phys. **5**, 209 (2014).

- [33] M. Randeria, W. Zwerger and M. Zwierlein, “The BCS-BEC Crossover and the Unitary Fermi Gas”, in Lecture Notes in Physics 836, Springer-Verlag Berlin Heidelberg 2012.
- [34] G. C. Strinati et. al., Phys. Rep **738**,1 (2018).
- [35] B.A. McKinney, M. Dunn, D.K. Watson, and J.G. Loeser, Ann. Phys. **310**, 56 (2003).
- [36] M. Dunn, D.K. Watson, and J.G. Loeser, Ann. Phys. (NY), **321**, 1939 (2006).
- [37] W.B. Laing, M. Dunn, and D.K. Watson, J. of Math. Phys. **50**, 062105 (2009).
- [38] D.K. Watson, Phys. Rev. A **93**, 023622 (2016).
- [39] D.K. Watson, Phys. Rev. A **92**, 013628 (2015).
- [40] D.K. Watson, J. Low Temp. Phys. **212**, 1 (2023).
- [41] D.K. Watson, J. Phys. B. **52**, 205301 (2019).
- [42] D.K. Watson, J. Low Temp. Phys. **221**, 108 (2025).
- [43] D.K. Watson, Phys. Rev. A **104**, 033320 (2021).
- [44] D.K. Watson, EPL **146**, 45002(2024).
- [45] A.J. Leggett, In *Modern Trends in the Theory of Condensed Matter. Proceedings of the XVIth Karpacz Winter School of Theoretical Physics, Karpacz, Poland*, pgs. 13-27, Springer-Verlag, Berlin, 1980.
- [46] A.J. Leggett, Rev. Mod. Phys. **73**, 307(2001).
- [47] D.M. Eagles, Phys. Rev. **186**, 456 (1969).
- [48] P. Nozieres and S. Schmitt-Rink, J. Low Temp. Phys. **59**, 195 (1985).
- [49] L. Salasnich, Phys. Rev A **72**, 023621(2005).
- [50] D.K. Watson, Ann.Phys. **419**, 168219 (2020).
- [51] M. Combescot et. al., Euro. Phys. J. B **80**, 41 (2011).
- [52] M. Crouzeix and M. Combescot, Phys. Rev. Lett. **107**, 267001 (2011).
- [53] W. Pogosov and M. Combescot, Physica C **471**, 566 (2011).
- [54] J. Bardeen, L.N. Cooper, and J.R. Schrieffer, Phys. Rev. **108**, 1175 (1957).
- [55] F. London, “Superfluids”,Wiley, New York, 1950.
- [56] F. London, Phys. Rev. **24**, 562 (1948).
- [57] J.R. Schrieffer, Science **180**, 1243 (1973).
- [58] G. t’Hooft, Nucl. Phys. **B72**, 461(1974);B75(1974).
- [59] K.G. Wilson, Phys. Rev. Lett. **28**, 548 (1972); Rev. Mod. Phys. **55**, 838 (1983).
- [60] G. Chen et.al., J. Math. Chem. **48**, 791(2010).
- [61] A.Svidzinsky et.al., International Reviews in Physical Chemistry, **27**, 665 (2008).
- [62] D.R. Herrick, J. Math. Phys. **16**, 281(1975).
- [63] J.G. Loeser et. al., J. Chem.Phys. **100**,5036(1994).
- [64] S. Kais and D.R. Herschbach, J. Chem. Phys. **100**, 4367(1994).
- [65] J.G. Loeser, J. Chem. Phys. **86**, 5635(1987).
- [66] D.R. Herschbach et. al., J. Phys. Chem. A **121**, 6336 (2017).
- [67] W.L. Virgo and D.R. Herschbach, Chem. Phys. Lett. **634**, 179(2015).
- [68] P.F. Loos and P.M.W. Gill, Phys. Rev. Lett. **105**, 113001(2010).
- [69] A. Svidzinsky et al., Phys. Today **66**, 33 (2014).
- [70] S. Kais et al., J. Phys. Chem. **98**, 11015(1994).
- [71] A. Svidzinsky et al., Phys. Rev. Lett. **95**, 080401 (2005).
- [72] A. Chatterjee, J. Math. Phys. **41**, 2515(2000).

- [73] Y.P. Varshni, Can. J. Phys. **71**, 122(1993).
- [74] S.M. Sung and J.M. Rost, J. Phys. Chem. **97**, 2479 (1993).
- [75] S. Kais and P. Serra, Adv. Chem Phys. **125**, 1(2003).
- [76] V.S. Popov, and A.V. Sergeev, Phys. Lett A **172**, 193(1993).
- [77] V.S. Popov and A.V. Sergeev, Phys. Lett. A. **193**, 165(1994).
- [78] S. Kais and D. R. Herschbach, J. Chem. Phys. **98**, 3990(1993).
- [79] K. Capelle and L.N. Oliveira, Phys. Rev B **73**, 113111 (2006).
- [80] W. Metzner and D. Vollhardt, Phys. Rev Lett. **62**, 324(1989).
- [81] K. G. Wilson and J. Kogut, Phys. Rev. C **12**, 75 (1974).
- [82] E. Whitten, Phys. Today **33**(7), 38(1980).
- [83] G. t’Hooft, “Large N”, arXiv:hep-th/0204069v1, (2002).
- [84] C.J. Ahn, J. High Energy Physics **125**(2011).
- [85] C. Rim and W.I. Weisberger, Phys. Rev. Lett. **53**, 965 (1984).
- [86] C. Bender and S. Boettcher, Phys. Rev. D **51**, 1875(1995).
- [87] M. Horacsu et. al., Nuclear Physics B **164**, 333(1980).
- [88] “The Large N Expansion in Quantum Field Theory and Statistical Physics”, E. Brezin and S.R. Wadia, eds. World Scientific Publ. Co, 1993.
- [89] B.A. McKinney et al., Phys. Rev. A **69**, 053611 (2004).
- [90] W.B. Laing et al., Phys. Rev. A **74**, 063605 (2006).
- [91] W.B. Laing et al., J Phys A **42**, 205307 (2009).
- [92] M. Dunn et al., Phys. Rev A **80**, 062108 (2009).
- [93] D.K. Watson, Phys. Rev. A **96**, 033601(2017).
- [94] Y. K. Liu et. al., Phys. Rev. Lett. **98**, 110503 (2007).
- [95] A. Montina, Phys. Rev. A **77**, 22104 (2008).
- [96] D.K. Watson and M. Dunn, Phys. Rev. Lett. **105**, 020402 (2010).
- [97] D.K. Watson and M. Dunn, J. Phys. B **45**, 095002 (2012).
- [98] W.B. Laing et al., EPAPS E-JMAPAQ-50-031904.
- [99] *Dimensional Scaling in Chemical Physics*, edited by D.R. Herschbach, J. Avery, and O. Goscinski (Kluwer, Dordrecht, 1992).
- [100] *New Methods in Quantum Theory*, edited by C. A. Tsipis, V. S. Popov, D. R. Herschbach, and J. Avery, NATO Conference Book, Vol. 8. (Kluwer Academic, Dordrecht, Holland).
- [101] S. Kais and D.R. Herschbach, J. Chem. Phys. **100**, 4367 (1994).
- [102] S. Kais and R. Bleil, J. Chem. Phys. **102**, 7472 (1995).
- [103] J. Avery et al., Theor. Chim. Acta **81**, 1 (1991).
- [104] E.B. Wilson, Jr., J.C. Decius, P.C. Cross, *Molecular vibrations: The theory of infrared and raman vibrational spectra*. McGraw-Hill, New York, 1955.
- [105] M. Hamermesh, *Group theory and its application to physical problems*, Addison-Wesley, Reading, MA, 1962.
- [106] See for example Ref. [104], Appendix XII, p. 347.
- [107] L.D. Landau, Sov. Phys. **3**,920(1956); *ibid.* **5**,101(1957).
- [108] J. Carlson and S. Gandolfi, Phys. Rev. A **90** 011601(R) (2014).
- [109] C. Sanner, L. Soncerhouse, R.B. Hutson, L. Yan, W.R. Milner and J. Ye, Science **374**, 979(2021).
- [110] A.B. Deb and Kjergaard, Science **374**, 972(2021).

- [111] Y. Margalit, Y-K Lu, F. Cagritop and W. Ketterle, *Science* **374**, 976(2021).
- [112] R. Jannin, Y. van der Werf, K. Steinebach, H.L. Bethlem and K.S. Eikema, *Nat. Commu.* **13**, 6479(2022).
- [113] R.B. Diener, R. Sensarma and M. Randeria, *Phys. Rev. A* **77**, 023626 (2008).
- [114] L. Salasnich and F. Toigo, *Physics Reports* **640**, 1 (2016).
- [115] N.A. Rodríguez-Briones, H. Katiyar, E. Martín-Martínez, and R. Laflamme, *Phys. Rev. Lett.* **130**, 110801 (2023).
- [116] S.Y. Chang and G.F. Bertsch, *Phys. Rev. A* **76**, 021603 (2007); N.T. Zinneret al., arXiv:0803.2861.
- [117] D. Blume, J. von Stecher, and C. H. Greene, *Phys. Rev. Lett.* **99**, 233201(2007).
- [118] J.T. Stewart, J.P. Gaebler, C.A. Regal and D.S. Jin, *Phys. Rev. Lett.* **97**, 220406 (2006).
- [119] S.K. Adhikari, *Phys. Rev. A* **79**, 023611 (2009).
- [120] R. Jáuregui, R. Paredes, and G. Toledo Sánchez, *Phys. Rev. A* **76**, 011604(R) (2007).